Flat, ferrocenyl-conjugated peptides: a combined electrochemical and spectroscopic study

Barbara Biondi,[a] Roberta Cardena,[b] Annalisa Bisello,[b] Renato Schiesari,[b] Laura Cerveson,[b] Martino Facci,[b] Marzio Rancan,[c] Fernando Formaggio[a,b] and Saverio Santi*[b]

In Memoriam of Prof. Jean-Michel Savéant

[a] Dr. B. Biondi, Prof. F. Formaggio
Institute of Biomolecular Chemistry, Padova Unit, CNR
via Marzolo 1, 35131 Padova, Italy
[b] Dr. R. Cardena, Dr. A. Bisello, Dr. R. Schiesari, Dr. Laura Cerveson, Dr. Martino Facci, Prof. F. Formaggio, Prof. S. Santi
Department of Chemical Sciences
University of Padova
via Marzolo 1, 35131 Padova, Italy
E-mail: saverio.santi@unipd.it
[c] Institute of Condensed Matter Chemistry and Technologies for Energy (ICMATE), CNR
Via Marzolo 1, 35131 Padova, Italy

Supporting information for this article is given via a link at the end of the document.

Abstract: We synthesized two homo-peptide series, based on the $C^{\alpha,\beta}$-didehydroalanine residue. One series was functionalized with a ferrocene (Fc) moiety at the N-terminus, the other series with a Fc at the C-terminus. These conjugates adopt the flat, fully-extended conformation, also known as 2.0_5-helix. Cyclic voltammetry measurements revealed that the peptide length does not affect the redox behavior of Fc, independently on the peptide end at which it is appended. This outcome perfectly fits with the presence of fully-extended peptides, as in this 3D-structure the dipole moment is negligible. Thus, we confirm the results of our previous study with two Fc pendants: fully-extended, α-peptide stretches prevent or reduce the charge transfer along the peptide chain.

Introduction

Electron/charge transfer in biological molecules is a crucial event for life.[1] In addition, by unraveling these natural mechanisms one can design systems with new functions, such as enzymatic fuel cells,[2] biosensors,[3] or bio-electrocatalysts.[4] To this aim, the study of simpler, synthetic peptides provides an easy-to-handle tool to access the mechanisms of electron transfer in proteins. Indeed, with small molecules it is easier to assign the role played, for instance, by H-bonds or dipole moments associated with helical peptides. In this connection, helical peptides are undoubtedly the most investigated molecules.[5,6] In particular, in α- and 3_{10}-helices the macro-dipole moment generated by the C=O alignment has been one of the most investigated features.[7] Because of this dipole, peptide helices can favor or counteract an electron transfer.[7] However, there exists an uncommon conformation able to prevent or reduce charge transfer along a peptide chain.[8] This 3D-structure, rarely observed in proteins,[9] is the *fully-extended* conformation. It is also termed 2.0_5-helix, as 2 residues are required to make a full turn (180° rotation per residue) and the stabilization is given by H-bonds forming pseudo-cycles of 5 atoms (Figure 1).[10] As a consequence, the 2.0_5-helix is flat and spans the longest N-to-C termini distance that an α-peptide can adopt. Interestingly, the C=O are aligned perpendicularly to the propagation direction of the 2.0_5-helix (Figure 1). Therefore, a macro-dipole moment is neither produced along the helix axis, nor perpendicularly to it as the single C=O dipoles have opposite orientations. This condition is dramatically diverging from that observed in α- or-3_{10}-helical peptides, where the amide C=O align along the helix axis and generate important macro-dipoles. In our recent contribution [8c] we have shown that the 2.0_5-helix has indeed a negligible dipole moment, thus confirming the relevance of this feature in promoting electron/charge transfer in helical peptides. In that contribution we appended two ferrocene (Fc) probes to the ends of flat peptides, as we previously did with 3_{10}-helical peptides.[11] However, we did not observe communication between the two Fc moieties,[8c] at variance from the case where the intervening peptides are 3_{10}-helices.[11]

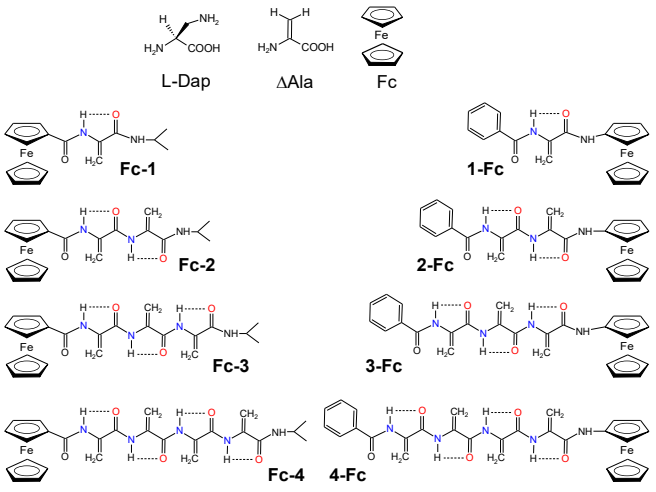

Figure 1. Chemical structures of the amino acids (Dap and ΔAla) and the electrochemical probe (Fc) used in this work (top) and of the peptides synthesized. Intra-residue H-bonds are indicated by dashed lines.

To validate our conclusion on the absence of an electron/charge conduction in the 2.0_5-helix, in this contribution we report a conformational and electrochemical study on two peptide series bearing only one Fc unit at the N- or C-peptide terminus (Figure 1). In α- or 3_{10}-helical peptides the electrochemical behavior of the probe is strongly affected by the length of the peptide and by the end (N or C) to which it is linked. In the present work, we expect both conditions to be insignificant because we used, as in Ref. 8c, the naturally occurring, $C^{\alpha,\beta}$-didehydroalanine (ΔAla) residue,[12] known to promote the 2.0_5-helix.[8a,8c,13] Again, we relied on Fc as electrochemical probe as its derivatives are stable in solution and in air and preserve their redox characteristics even when chemically modified.[14] Also, Fc already proved to be a reliable probe in studies involving peptides.[6b,6f,6h,6m,8c,11,15]

Results and Discussion

Peptide synthesis

The synthesis of the two Fc/peptide series (Figure 1), namely Fc-CO-(ΔAla)$_n$-NH-*i*Pr (*n* = 1-4; *i*Pr = isopropyl) and Bz-(ΔAla)$_n$-NH-Fc (*n* = 1-4; Bz = benzoyl, was carried out according to previously reported strategies.[8,13] In particular, we first synthesized the precursor peptide series containing Dap (2,3-diaminopropionic acid, Figure 1). This residue was then converted into ΔAla by performing the Hoffman elimination.

Yields were from good to acceptable, depending on the length of the peptides and their solubility. When necessary, purification *via* medium pressure chromatography was applied. Characterization data are given as Supporting Information.

Conformational analysis

We investigated by means of NMR and IR absorption spectroscopies the conformation of our Fc/peptides in $CDCl_3$ solution. The IR spectra (Figure 2) suggest the adoption for both series of the fully-extended conformation (2.0_5-helix), stabilized by *intra-residue* H-bonds.

In the amide A region (Figure 2A and 2C) the band at about 3440 cm^{-1} is due to the stretching of C-terminal amide N-H, not involved in H-bonds. The intense band at about 3385 cm^{-1}, that encompasses all other amide NH, has the typical frequency of the *intra*-residue (C_5 conformation) H-bond observed in ΔAla peptides.[8a,8c,13] In addition, in all peptides this frequency is unchanged, because the intra-residue H-bonds in the 2.0_5-helix do not interconnect with residues that precede or follow. As a matter of fact, in α(or 3_{10})-helical peptides, this band shifts to lower frequencies by lengthening the chain as a cooperative H-bond pattern increase the helix stability.

In the amide I and amide II regions (Figure 2B ad 2D) we observe additional features typical of the 2.0_5-helix: (i) the band of the amide I (~1660 cm^{-1}) is less intense than that of the amide II (~1500 cm^{-1}), whereas in α- and 3_{10}-helices the opposite is true; (ii) the amide II band is located below 1500 cm^{-1}, as observed only in 2.0_5-helices.[10f-i] Finally, the shift to lower frequencies of the amide II absorption when the peptide length increases may be attributed to (alkene)C-H···O=C electrostatic interactions, clearly observed in crystal-state structures.[8c,13] Indeed, the amide C-N stretching, that is contributing up to 40% to the amide II band, is favored if the amide C=O is weakened by an additional H-bond with an alkene.

The NMR conformational analysis, performed in the same solvent, corroborates the conclusions drawn from the IR absorption spectra. To completely assign all the ^{1}H resonances we took advantage of homo-nuclear 2D-experiments. In addition, this work allowed us to detect a pattern of connectivity typical of a fully-extended conformation[10f] for both peptide series.

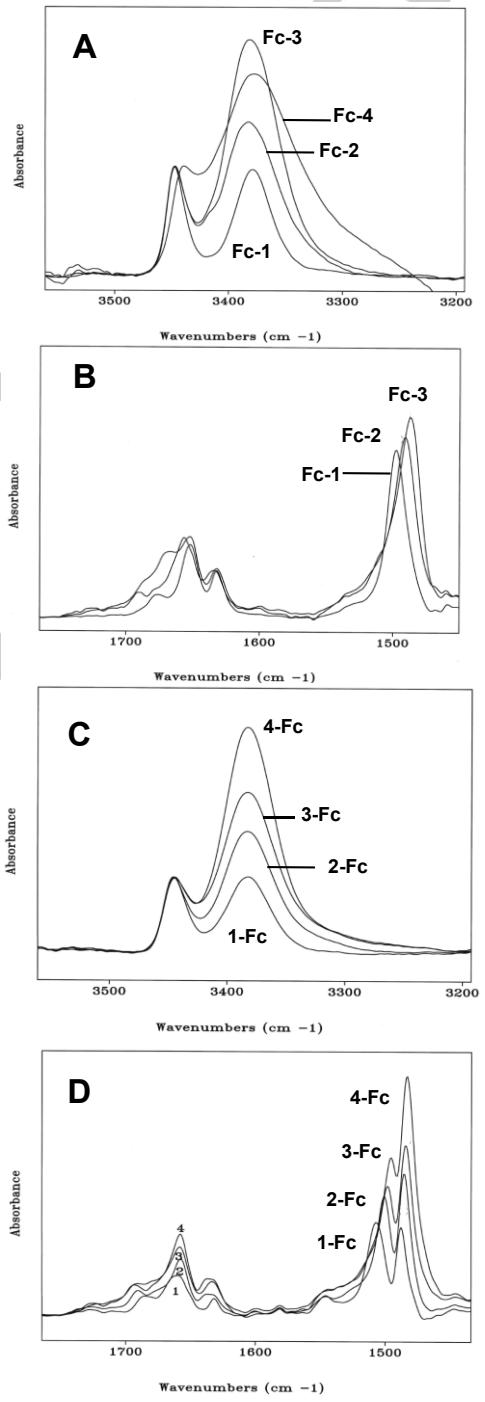

Figure 2. FT-IR absorption spectra of Fc-CO-(ΔAla)$_n$-NH-*i*Pr (*n* = 1,4; A and B) and Bz-(ΔAla)$_n$-NH-Fc (*n* = 1,4; C and D) in the amide A (3500-3200 cm^{-1}) and amide I and II (1700-1450 cm^{-1}) regions. Peptide concentration: 1 mM in $CDCl_3$. Due to the peptide low solubility in $CDCl_3$, the spectrum of **Fc-4** was recorded in CH_2Cl_2 solution. As a consequence, the absorption of the solvent hampers a reliable recording of the spectrum for **Fc-4** in the carbonyl region.

As a representative example we report a section of the NOESY spectrum of Bz-(ΔAla)$_4$-NH-Fc (Figure 3). As we previously reported for ΔAla homo-peptides bearing two Fc moieties,[8c] here too we observe all the cross peaks between an H of the ΔAla β-CH$_2$ and the proton N-H of the following residue. We also detect an interaction between an aromatic C-H of the N-terminal benzoyl and the N-H of ΔAla$_1$ and a connectivity between a β-CH$_2$ H of the C-terminal ΔAla and the N-H linked to Fc.

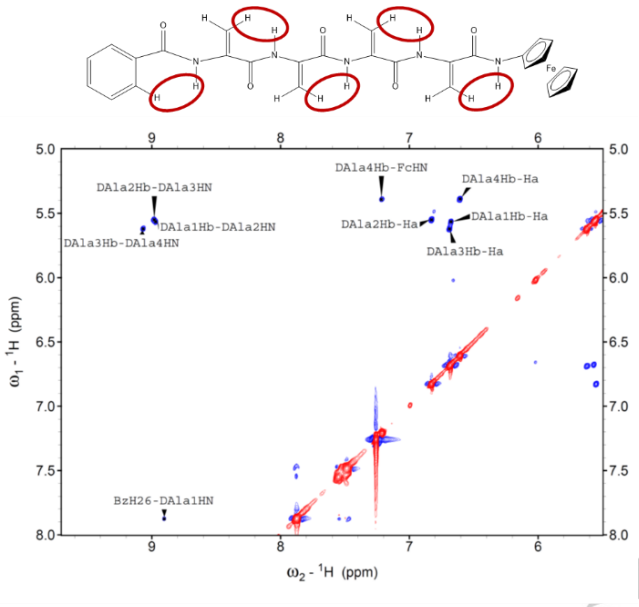

Figure 3. βCH→NH region of the NOESY spectrum of Bz-[ΔAla]$_4$-NHFc in $CDCl_3$ solution, T=25°C.

The same pattern of interactions was observed also for the Fc-CO-(ΔAla)$_n$-NH-*i*Pr (*n* = 1-4) series. In all peptides we found the cross-peaks characteristics of the C5-conformation (βCH$_{2(i-1)}$/NH$_{(i)}$ connectivities) together with a correlation between the αC-H of the N-terminal Fc moiety and the N-H of ΔAla$_1$. A section of the NOESY spectrum of the tetrapeptide is reported in Figure 4.

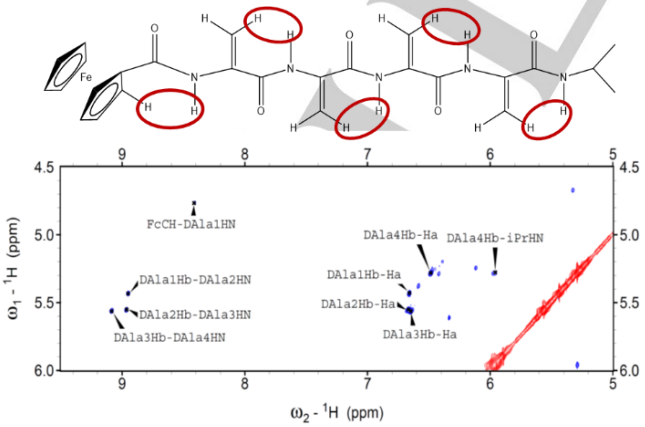

Figure 4. βCH→NH region of the NOESY spectrum of Fc-CO-(ΔAla)$_4$-NH-*i*Pr in $CDCl_3$ solution, T=25°C.

We were also able to grow a single crystal of Bz-ΔAla-NH-Fc (**1-Fc**), suitable for X-ray diffraction analysis. The molecular structure of **1-Fc** is illustrated in Figure 5. In terms of bond lengths and angles, the compound has very similar features to those previously reported for the same C$^{\alpha}$,C$^{\beta}$ unsaturated residue.[8c,9a,13] In particular, the fully-extended conformation is stabilized by two H-bonds (Table S1). One involves N1−H1 and C1=O1, thus forming a five-membered *pseudo*cycle (C_5 structure). The H1···O1 distance is 2.107 Å, and the value of the N1−H1···O1 angle is 112.79°. Even if N−H···O=C interactions with N−H···O angles less than 120° are not usually considered to be H-bonds, there are spectroscopic and computational evidence for the H-bond nature of the these *pseudo*cycles.[9] The second H-bond involves as the donor a H atom of the ΔAla β-CH$_2$ group and the preceding carbonyl oxygen atom as the acceptor (length H1BA···O0A = 2.383 Å, angle C1B−H1BA···O0A = 119.72°). Finally, NT-HT and O0A are involved in an array of intermolecular H-bonds that supports the crystallographic packing (Figure S5).

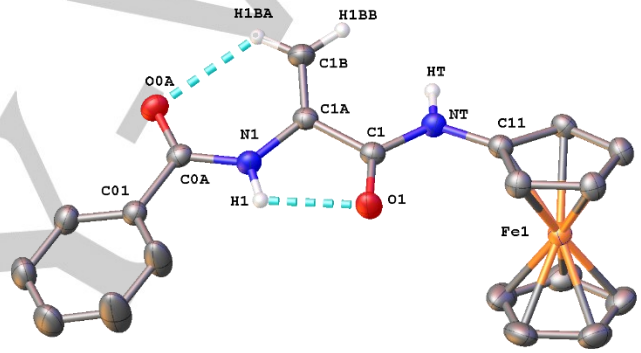

Figure 5. X-Ray diffraction structure of Bz−ΔAla−NH−Fc (**1-Fc**) with atom numbering. Anisotropic displacement ellipsoids for the non-H atoms are displayed at the 30 % probability level. H-atoms of the ferrocene unit and benzyl ring are omitted for clarity. The intramolecular N−H···O=C and C−H···O=C H-bonds are indicated by dashed lines.

Cyclic voltammetry

Electrochemical investigations on peptide conjugates containing a terminal ferrocene Fc unit allowed to obtain information on the effect of the secondary structure and the length of the peptide chains.[8c,11] In particular, in this work cyclic voltammetry measurements have been carried out on the series Bz-(ΔAla)$_n$-NH-Fc (*n* = 1-4) and Fc-CO-ΔAla$_n$-NH-*i*Pr (*n* = 1-4). Similar studies were previously reported by some of us[11] on homopeptides of α-amino isobutyric acid (Aib) conjugated with Fc units. For peptides conjugated at the C-terminus, Z-(Aib)$_n$-NH-Fc (A$_n$ *n* = 1-5), and at the N-terminus, Fc-CO-(Aib)$_n$-OMe (B$_n$ *n* = 1-5), it was noted that the variation of the oxidation potentials depends on the position of the Fc group. In fact, the orientation of the peptide macrodipole (Figure 6), whose intensity increases as the number Aib residues increases, makes it easier to oxidize Fc (less positive potentials) along the A$_n$ series and more difficult (more positive potentials) along the B$_n$ series (Figure 7).

The oxidation of the Fc-NH-CO- group occurs at a lower potential than that of the Fc-CO-NH- group. The greatest effect of the macrodipole is observed in the tripeptide and this is due to the presence of two intramolecular H-bonds, C=O···N–H, which

stabilize the formation of an incipient 3_{10}-helix, compacting the structure and inducing maximum efficiency in the charge transfer process.

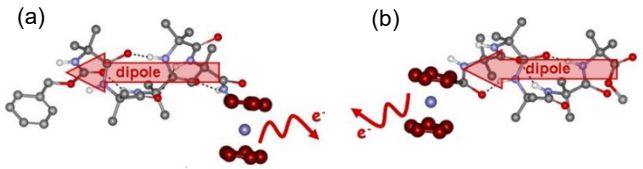

Figure 6. Macrodipole representation in (a) Z–(Aib)$_n$–NH–Fc (A_5) and (b) Fc–CO–(Aib)$_n$–OMe (B_5). Reprinted with permission from Ref. 11a. Copyright (2021).

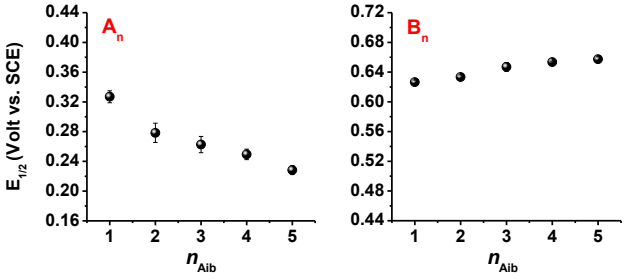

Figure 7. Oxidation potential variation of Z–[Aib]$_n$–NH–Fc (A_n, n=1–5) and Fc–CO–(Aib)$_n$–OMe (B_n, n=1–5). Reprinted with permission from Ref. 11a. Copyright (2021).

Dielectric (impedance) spectroscopy measurements made it possible to experimentally estimate the dipole moment of a series of Aib homopeptides in solution,[16] showing that the dipole moment increases linearly with the number of Aib units.

The results of the cyclic voltammetry analysis on the two planar peptide series here investigated are reported in Figure 8. Voltammograms, recorded under argon in CH_2Cl_2/nBu$_4$NPF$_6$ 0.1 M, show single oxidation waves of the Fc unit, monoelectronic, chemically reversible and nernstian in the scan rate range v between 0.1 and 5 Vs^{-1}, as well as standard ferrocene in the same conditions, on electrode gold disc working with diameter d = 0.125 mm (0.5–5 Vs^{-1}) and 0.5 mm (0.1–0.5 Vs-^{1}). The peak-to-peak separation is insensitive to the peptide elongation in both series, indicating that the heterogeneous electron transfer rate (k_{ET}) does not depend on the ΔAla number in the chains.

The difference in peak current intensity (i_{max}) among the voltammograms of each peptide series is due to the difference in the diffusion coefficients (D) as the number of residues varies, considering that the relative diffusion coefficients depend on the molecular size, according to the Stokes-Einstein equation (D ∝ 1/r). In fact, for a Nernstian electron transfer process, the i_{max} value of a cyclic voltammetry experiment is given by the equation:[17]

$$i_{max} = (2.69\times10^5)n^{3/2}CAD^{1/2}v^{1/2}$$

where A is the area of the electrode, D the diffusion coefficient, C the concentration of the electroactive species, v the potential scan rate and n the number of electrons exchanged. Lower values of D are expected for longer and functionalized peptides. In fact, since it is a fluid-dynamic effect, it is linked to the different dimensions of the molecules and their mobilities, lower for the larger ones, towards the electrode.

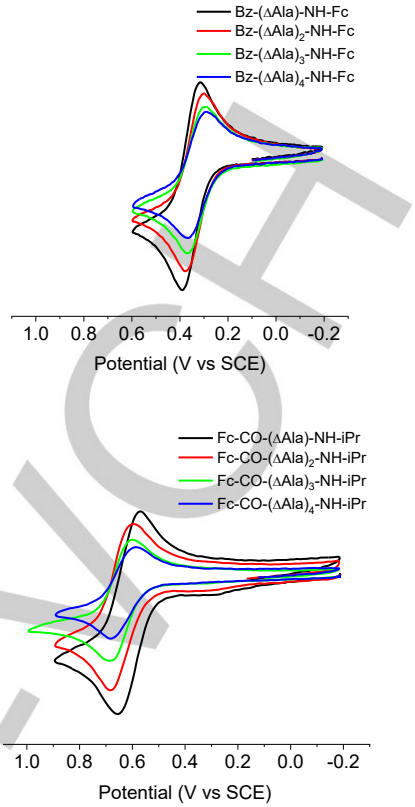

Figure 8. CVs of Bz–(ΔAla)$_n$–NH-Fc and Fc–CO–(ΔAla)$_n$–NH–iPr (n=1–4). Gold disk gold electrode d=0.5 mm, solvent CH_2Cl_2/nBu$_4$NPF$_6$ 0.1 M, scan rate v=0.2 Vs^{-1}; c=1–3 mM. Current i is normalized according to equation $iv^{-1/2}C^{-1}A^{-1}$.

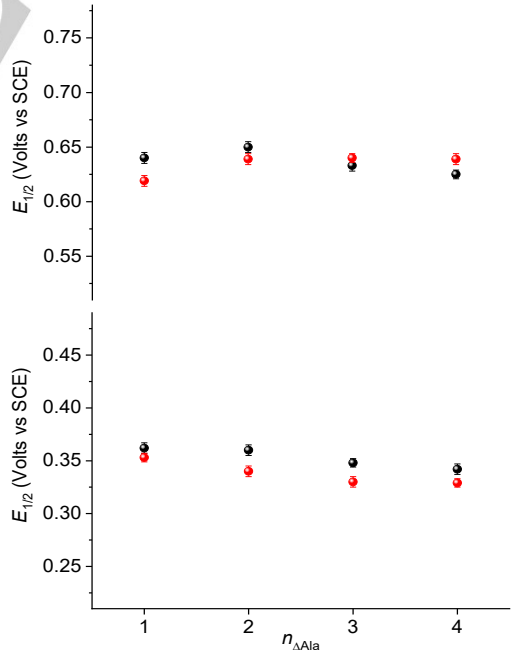

Figure 9. Oxidation potential variation of Bz-(ΔAla)$_n$-NH-Fc (red open circles), Fc–CO-(ΔAla)$_n$–NH–iPr (red full circles) and Fc–CO-(ΔAla)$_n$–NH–Fc (black full and open circles). $E_{1/2}$ ± $\delta E_{1/2}$ values were obtained by replicated series of experiments with $\delta E_{1/2}$ = 4÷5 mV.

The graphics in Figure 9 shows the trend of the oxidation potentials of the two, mono-Fc series here investigated as a function of the number of ΔAla residues. For comparison, the oxidation potential values of the peptides of the bis-Fc end-capped series, Fc-CO-$(\Delta Ala)_n$-NH-Fc (n = 1–4), are reported.[8c] Unlike the Aib peptides (3_{10}-helix), which manifested clear-cut dependence of the potential on the peptide length, in this case the variation of the potential is minimal and is null as the $(\Delta Ala)_n$ chain increases, thus suggesting that the prolonged H-bond networks confer more stiffness to the backbone. This effect is clearly related to the fully-extended conformation of the peptides (2.0_5-helix), where the orientation of the carbonyl groups does not produce a peptide macrodipole. The same conclusion was obtained with a ΔAla series having as N-terminus a *para*-cyanobenzoil.[8a]

Vis-MIR chemical oxidation

To verify the formation of oxidized species and to study the eventual propagation of the charge along the peptide chain, visible (Figure 10) and IR spectra, in the amide A (Figures 11 and 12) and carbonyl (Figures 13 and 14) regions of the Bz-$(\Delta Ala)_n$-NH-Fc^+ and Fc-CO-$(\Delta Ala)_n$-NH-*i*Pr^+ ions were analyzed and compared to those of the neutral peptides. Stable solutions were obtained by chemical oxidation of the neutral peptides in CH_2Cl_2 solution, by incremental addition of the oxidizing agents, ferrocenium[BF_4] (up to 1 equivalent).

In particular, during oxidation of Bz-$(\Delta Ala)_n$-NH-Fc the typical absorption band at 752–760 nm (visible region) of a -NH-Fc^+ group is observed. Similarly, the oxidation of Fc-CO-$(\Delta Ala)_n$-NH-*i*Pr produced an absorption band around 620 nm, characteristic of a Fc^+-CO- group.[11b] As an example, in Figure 10 the visible spectra for the stepwise oxidation of Bz-$(\Delta Ala)_2$-NH-Fc and Fc-CO-$(\Delta Ala)_2$-NH-*i*Pr are shown.

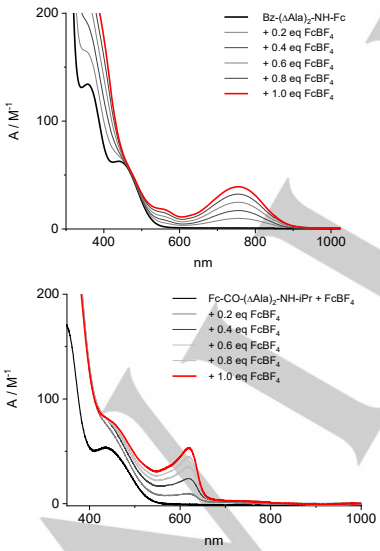

Figure 10. Visible absorption spectra in CH_2Cl_2 of (a) Bz–$(\Delta Ala)_2$–NH-$Fc^{0/+1}$ and (b) Fc–CO$(\Delta Ala)_2$–NH–i$Pr^{0/+1}$ obtained by oxidation of the neutral parent compounds up to 1 equivalent of ferrocenium[BF_4] as the oxidizing agent.

The presence of a positive charge on the Fc moiety of Bz-$(\Delta Ala)_n$-NH-Fc (Figure 11) caused a dramatic shift of the band of the amide N−H directly linked to Fc^+ (NH_{Fc}) from 3440 cm^{-1} to below 3300 cm^{-1}. On the contrary, the band at 3380 cm^{-1} related to intra-residue, H-bonded N-H is insensitive to the charge. We attribute this behaviour to the presence of a 2.0_5-helix as in this type of structure Fc is not connected to the peptide amides through H-bonds. In Fc-CO-$(\Delta Ala)_n$-NH-*i*Pr^+ cations (Figure 12), both the bands related to the $NH_{iPr/free}$ at 3440–3442 cm^{-1} and the $NH_{pept/H\text{-}bond}$ at 3408–3380 cm^{-1} are unaffected by the injection of the positive charge. Again, the amide N-Hs have no H-bond communication with Fc because the peptides are fully-extended.

These spectroscopic results, together with the electrochemical outcomes, are in favour of a charge-protecting nature of $(\Delta Ala)_n$ peptides, particularly efficient when the peptide length increases. Contrary to what has been observed for the Fc-conjugated $(Aib)_n$ peptides,[11] in which the effect of the positive charge on the farthest free amide NH is transmitted even for n = 5, in the $(\Delta Ala)_n$ series the charge is localized on the Fc groups, as suggested by the huge low-energy shift (~160 cm^{-1}) of the NH_{Fc} band.

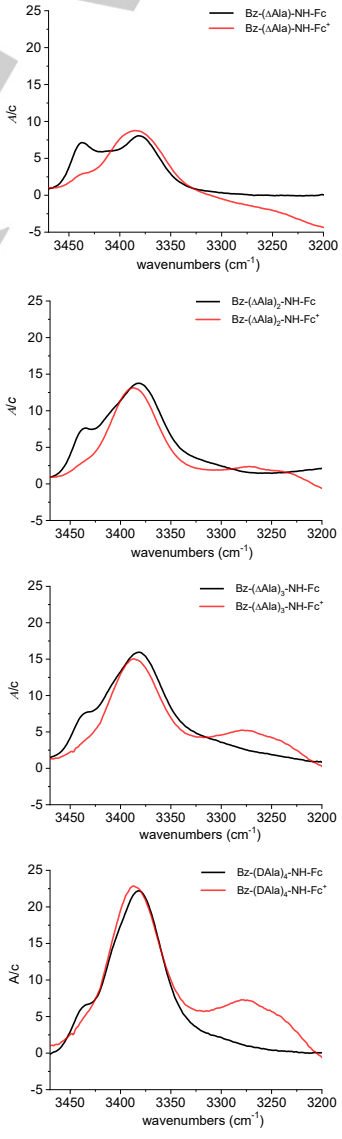

Figure 11. IR absorption spectra in the N−H stretching region of Bz–$(\Delta Ala)_n$–NH–$Fc^{0/+}$ (n=1–4). Solvent CH_2Cl_2.

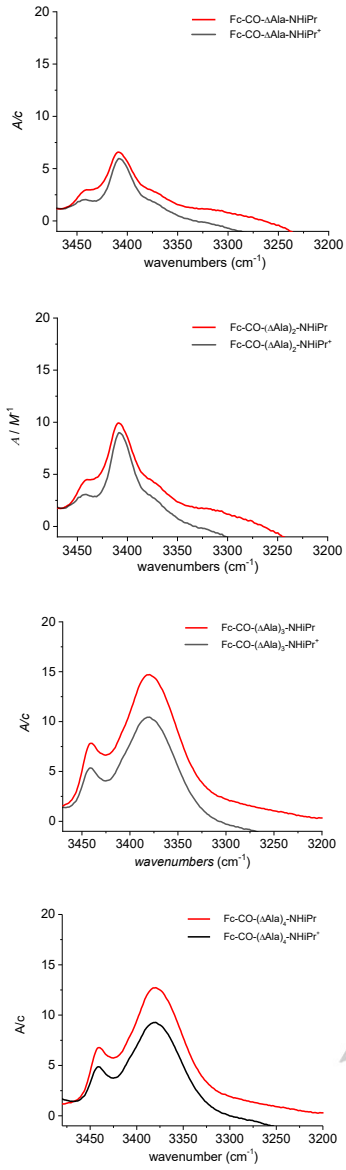

Figure 12. IR absorption spectra in the N−H stretching region of Fc–CO–$(\Delta Ala)_n$–NH–$iPr^{0/+}$ (n=1–4). Solvent CH_2Cl_2.

Conclusion

In this work we corroborated the finding of previous studies[8] in which a flat, fully-extended α-peptide was used as mediator of electron/charge transfer. We recently functionalized these peptides with two Fc moieties at their ends.[8c] We observed a lack of communication between the two Fc units. This result is in agreement with the spatial arrangement of the amide C=O in a fully-extended peptide: they do not sum up to generate a dipole moment. However, to exclude the presence of mutually erasing interactions among the two Fc, in this work we synthesized and studied two homo-peptide series bearing only one Fc, at the N- or at the C-terminus. We were able to confirm that the peptide length has no or slight influence on the redox behavior of Fc, because in a fully-extended peptide the dipole moment is absent. Therefore, this type of peptides can be exploited as spacers, not able to transfer charges as α- and 3_{10}-helices do.

Experimental Section

Synthesis. Experimental procedures for the synthesis of the Fc-conjugated peptides and their characterization data are reported in the Supporting Information.

UV-Vis analysis. Solution absorption spectra in the UV-vis region were recorded at 293 K with a JASCO V770 double beam spectrophotometer using quartz cells with 2 mm optical path. A solution of CH_2Cl_2 (baseline) spectra was recorded under the same conditions. Oxidation was achieved in an air-tight container connected to a vacuum/argon line by incremental addition of oxidizing agent solution (ferrocenium[BF_4]/CH_2Cl_2) from 0.2 to 1.0 equivalents. HPLC grade CH_2Cl_2 ≥ 99% was purchased from Carlo Erba and distilled on CaH_2 (≥ 97% powder Sigma Aldrich).

FT-IR analysis. Solution FT-IR absorption spectra were recorded at 293 K using a FT-IR Nicolet Nexus 670 spectrophotometer, nitrogen flushed, equipped with a sample-shuttle device, at 2 cm^{-1} nominal resolution, averaging 25 scans. Solvent (baseline) spectra were recorded under the same conditions. Spectrograde $CHCl_3$-d_1 (99.8%, d) was purchased from Sigma Aldrich. For spectral elaboration, the software SpectraCalc provided by Galactic (Salem, MA) was employed. Cells with path lengths of 1.0 and 10 mm (with CaF_2 windows) were used.

Nuclear Magnetic Resonance. ^{1}H spectra were obtained on a Bruker Avance III HD spectrometer operating at 400.13 (T = 298 K). The peptide concentration in solution was 1 mM in spectrograde $CHCl_3$-d_1 (99.8 % d_1 containing 0.5 %wt. of silver foils as stabilizers and 0.03 % (v/v) tetramethylsilane - Sigma Aldrich) and DMSO-d_6 (99.96% D-Eurisotop). Processing and evaluation of the experimental data were carried out using the TOPSPIN software packages. All homonuclear spectra were acquired by collecting 400 experiments, each consisting of 32 scans and 2K data points. The spin systems of the amino acid residues were identified using standard chemical shift correlation and 2D (NOESY, TOCSY and COSY) experiments.

X-Ray diffraction. Crystals of **1-Fc** were grown by slow evaporation from a chloroform solution. Data were collected using an Oxford Diffraction Gemini E diffractometer, equipped with a 2K × 2K EOS CCD area detector and sealed–tube Enhance (Mo) and (Cu) X–ray sources. A single crystal was mounted by fastening it on a nylon loop and measuring at room temperature. Detector distance was set at 45 mm. The diffraction intensities were corrected for Lorentz/polarization effects as well as with respect to absorption. Empirical multi-scan absorption corrections using equivalent reflections were performed with the scaling algorithm SCALE3 ABSPACK. Data reduction, finalization and cell refinement were carried out through the CrysAlisPro software. Accurate unit cell parameters were obtained by least squares refinement of the angular settings of strongest reflections, chosen from the whole experiment. The structure was solved with Olex2[18] by using ShelXT[19] structure solution program by Intrinsic Phasing and refined with the ShelXL[20] refinement package using least-squares minimization. In the last cycles of refinement, non-hydrogen atoms were refined anisotropically. Hydrogen atoms were included in calculated positions, and a riding model was used for their refinement. Deposition Number [2088623] contain the supplementary crystallographic data for this paper. These data are provided free of charge by the joint Cambridge Crystallographic Data Centre and Fachinformationszentrum Karlsruhe Access Structures service www.ccdc.cam.ac.uk/structures.

Bz−ΔAla−NH−Fc (**1-Fc**): $C_{20}H_{18}FeN_2O_2$ (M =374.21 g/mol): monoclinic, space group $P2_1/c$ (no. 14), a = 12.4786(3) Å, b = 9.9731(2) Å, c = 13.8673(3) Å, β = 98.609(2)°, V = 1706.34(7) Å^3, Z = 4, T = 297.5(3) K, μ(Mo Kα) = 0.899 mm^{-1}, *Dcalc* = 1.457 g/cm^3, 20324 reflections measured (7.212° ≤ 2Θ ≤ 58.508°), 4179 unique (R_{int} = 0.0272, R_{sigma} = 0.0210) which were used in all calculations. The final R_1 was 0.0357 (I > 2σ(I)) and wR_2 was 0.1018 (all data).

Cyclic voltammetry. The experiments were performed in an air-tight three-electrode cell connected to a vacuum/argon line. The reference electrode was a SCE (Tacussel ECS C10) separated from the solution by a bridge compartment filled with the same solvent/supporting electrolyte solution used in the cell. The counter electrode was a platinum spiral with around 1 cm^2 apparent surface area. The working electrode was a disk obtained from cross section of a gold wire with 0.5 and 0.125 mm diameter sealed in glass. Between successive scans, the working electrode was polished on alumina according to standard procedures and sonicated before use. An EG&G PAR-175 signal generator was used. The currents and potentials were recorded on a Lecroy 9310L oscilloscope. The potentiostat was home-built with a positive feedback loop for compensation of the ohmic drop.[21]

Acknowledgements

S.S. acknowledge the University of Padova for having supported this work through Grant P-DiSC-2018. B.B. and F.F. is grateful to the joint support from Fresenius Kabi iPSUM and the University of Padova (Grant Uni-Impresa 2019, PEPTIND).

Keywords: • dehydroalanine • dipole moment • ferrocene • flat peptides

[1] a) P. Hapiot, L. D. Kispert, V. V. Konovalov, J. M. Savéant, *J. Am. Chem. Soc.* **2001**, *123*, 6669–6677; b) T. P. Min, M. K. Eidsness, T. Ichiye, C. H. Kang, *J. Microbiol.* **2001**, *39,* 149-153; b) F. Maran, C. Toniolo, *Biopolymers (Pept. Sci.)* **2012**, *100*, III-IV, Editorial; c) M. Su, L. Roland, *ChemElectroChem* **2019**, *6*, 958-975; d) A. Ranieri, C. A. Bortolotti, G. Di Rocco. G. Battistuzzi, M. Sola, M. Borsari, *ChemElectroChem* **2019**, *6*, 5172-5185; e) F. Calisto, F. M. Sousa, F. V. Sena, P. N. Refojo, M. M. Pereira, *Chem. Rev.* **2021**, *121*, 1804-1844; f) M. Sarewicz, S. Pintscher, R. Pietras, A. Borek, L. Bujnowicz, G. Hanke, W. A. Cramer, G. Finazzi, A. Osyczka, *Chem. Rev.* **2021**, *121*, 2020-2108;

[2] a) J. Huang, P. Zhao, X. Jin, Y. W. Wang, H. T. Yuan, X. Y. Zhu, *Mater. Sci.* **2020**, *8,* 5230-5240; b) S. Y. Yu, N. V. Myung, *Front. Chem.* **2021**, *8*, Art. N. 620153. Biofuel cells

[3] L. Zuccarello, C. Barbosa, S. Todorovic, C. M. Silveira, *Catalysts* **2021**, *11*, Art. N. 218.

[4] T. Adachi, Y. Kitazumi, O. Shirai, K. Kano, *Catalysts* **2020**, *10,* Art. N. 1413.

[5] a) A. Shah, B. Adhikari, S. Martic, A. Munir, S. Shahzad, K. Ahmad, H.-B. Kraatz, *Chem. Soc. Rev.* **2015**, *44*, 1015-1027; b) N. Amdursky, *ChemPlusChem* **2015**, *80*, 1075-1095.

[6] a) V. I. Vullev, G. Jones, *Res. Chem. Intermediat.* **2002**, *28,* 795-815; b) T. Morita, S. Kimura, *J. Am. Chem. Soc.* **2003**, *125*, 8732-8733; c) S. Antonello, F. Formaggio, A. Moretto, C. Toniolo, F. Maran, *J. Am. Chem. Soc.* **2003**, *125*, 2874-2875; d) R. Improta, S. Antonello, F. Formaggio, F. Maran, N. Rega, V. Barone, *J. Phys. Chem. B* **2005**, *109*, 1023-1033; e) F. Polo, S. Antonello, F. Formaggio, C. Toniolo, F. Maran, *J. Am. Chem. Soc.* **2005**, *127*, 492-493; f) K. Kitagawa, T. Morita, S. Kimura, *J. Phys. Chem. B* **2005**, *109*, 13906-13911; g) E. Gatto, L. Stella, F. Formaggio, C. Toniolo, L. Lorenzelli, M. Venanzi, *J. Pept. Sci.* **2008**, *14*, 184-191; h) S.Okamoto, T. Morita, S.Kimura, *Chem. Lett.* **2009**, 38, 126-127; i) E. Gatto, L. Stella, C. Baldini, C. Toniolo, F. Formaggio, M. Venanzi, *Superlattices Microstruct.* **2009**, *46*, 34-39; j) Y. Arikuma, H. Nakayama, T. Morita, S. Kimura, *Langmuir* **2011**, *27*, 1530-1535; k) L. Garbuio, S. Antonello, I. Guryanov, Y. J. Li, M. Ruzzi, N. J. Turro, F. Maran, *J. Am. Chem. Soc.* **2012**, *134*, 10628–10637; l) S. Mehlhose, N. Frenkel, H. Uji, S. Hölzel, G. Müntze, D. Stock, S. Neugebauer, A. Dadgar, W. Abuillan, M. Eickhoff, S. Kimura, M. Tanaka, *Adv. Funct. Mater.* **2018**, *28*, 1704034; m) D. Matsushita, H. Uji, S. Kimura, *Phys. Chem. Chem. Phys.*, **2018**, *20*, 15216-15222; n) C. Zuliani, F. Formaggio, L. Scipionato, C. Toniolo, S. Antonello, F. Maran, *ChemElectroChem* **2020**, *7*, 1225-1237.

[7] a) E. Galoppini, M. A. Fox, *J. Am. Chem. Soc.* **1996**, *118*, 2299-2300; b) M. A. Fox, E. Galoppini, *J. Am. Chem. Soc.* **1997**, *119*, 5277-5285; c) S. Yasutomi, T. Morita, Y. Imanishi, S. Kimura, *Science* **2004**, *304*, 1944-1947; d) S. Yasutomi, T. Morita, S. Kimura, *J. Am. Chem. Soc.* **2005**, *127*, 14564-14565; e) J. K. Hoober, L. L. Eggink, M. Chen, *Photosynth. Res.* **2007**, *94*, 387-400; f) E. Gatto, A. Porchetta, L. Stella, I. Guryanov, F. Formaggio, C. Toniolo, B. Kaptein, Q. B. Broxterman, M. Venanzi, *Chem. Biodivers.* **2008**, *5*, 1263-1278; g) E. Gatto, M. Caruso, A. Porchetta, C. Toniolo, F. Formaggio, M. Crisma, M. Venanzi, *J. Pept. Sci.* **2011**, *17*, 124-131; h) M. Lauz, S. Eckhardt, K. M. Fromm, B. Giese, *Phys. Chem. Chem. Phys.* **2012**, *14*, 13785-13788; i) E. Gatto, M. Venanzi, *Polym. J.* **2013,** *45*, 468-480; j) E. Gatto, M. Venanzi, *Isr. J. Chem.* **2015**, *55*, 671- 681; k) P. Gobbo, S. Antonello, I. Guryanov, F. Polo, A. Soldà, F. Zen, F. Maran, *ChemElectroChem* **2016**, *3*, 2063-2070; l) X. F. Song, Y. X. Bu, *PhysChemChemPhys* **2021**, *23*, 1464-1474.

[8] a) C. Toniolo, M. Crisma, C. Peggion, F. Maran, S. Antonello, F. Maran, R. Improta, V. Barone, Y. Tsuji, Y. Yamaguchi, T. Wakamiya in *Peptides 2006*, Proceedings of The Twenty-Ninth European Peptide Symposium (Eds.: K. Rolka, P. Rekowski and J. Silberring), Kenes International, Gdansk **2006**, pp. 770–771; b) R. Lettieri, M. Bischetti, E. Gatto, A. Palleschi, E. Ricci, F. Formaggio, M. Crisma, C. Toniolo, M. Venanzi, *Biopolymers (Pept. Sci.)* **2013**, *100*, 51-63; c) S. Santi, A. Bisello, R. Cardena, S. Tomelleri, R. Schiesari, B. Biondi, M. Crisma, F. Formaggio, *ChemPlusChem* **2021**, *86*, 723-730.

[9] a) M. Crisma, F. Formaggio, C. Alemán, J. Torras, C. Ramakrishnan, N. Kalmankar, P. Balaram, C. Toniolo, *Pept. Sci.* **2018**, *110*, e23100; b) R. W. Newberry, R. T. Raines, *Nat. Chem. Biol.* **2016**, *12*, 1084-1088.

[10] a) C. Peggion, A. Moretto, F. Formaggio, M. Crisma, C. Toniolo, *Biopolymers* **2013**, *100*, 621-636; b) M. Tanaka, S. Nishimura, M. Oba, Y. Demizu, M. Kurihara, H. Suemune, *Chem. Eur. J.* **2003**, *9*, 3082-3090; c) K. A. H. Wildman, A. Ramamoorthy, T. Wakamiya, T. Yoshikawa, M. Crisma, C. Toniolo, F. Formaggio, *J. Pept. Sci.* **2004**, *10*, 336-341; d) M. Tanaka, *Chem. Pharm. Bull.* **2007**, *55*, 349-358; d) M. Crisma, A. Moretto, C. Peggion, L. Panella, B. Kaptein, Q. B. Broxterman, F. Formaggio, C. Toniolo, *Amino Acids* **2011**, *41*, 629-641; e) F. Formaggio, M. Crisma, C. Peggion, A. Moretto, M. Venanzi, C. Toniolo, *Eur. J. Org. Chem.* **2012**, 167-174; f) C. Peggion, M. Crisma, C. Toniolo, F. Formaggio, *Tetrahedron* **2012**, *68*, 4429-4433; g) F. Formaggio, M. Crisma, G. Ballano, C. Peggion, M. Venanzi, C. Toniolo, *Org. Biomol. Chem.* **2012**, *10*, 2413–2421; h) H. Maekawa, G. Ballano, C. Toniolo, N.-H. Ge, *J. Phys. Chem. B* **2011**, *115*, 5168-5182; i) H. Maekawa, G. Ballano, F. Formaggio, C. Toniolo, N.-H. Ge, *J. Phys. Chem. C* **2014**, *118*, 29448-29457.

[11] a) A. Donoli, V. Marcuzzo, A. Moretto, C. Toniolo, R. Cardena, A. Bisello, S. Santi, *Org. Lett.* **2011**, *13*, 1282-1285; b) A. Donoli, V. Marcuzzo, A. Moretto, M. Crisma, C. Toniolo, R. Cardena, A. Bisello, S. Santi, *Pept. Sci.* **2012**, *100*, 14-24.

[12] a) D. Siodlak, *Amino Acids* **2015**, *47*, 1-17; b) S. Wang, Q. Fang, Z. Lu, Y. L. Gao, L. Trembleau, R. Ebel, J. H. Andersen, C. Philips, S. Law, H. Deng, *Angew. Chem. Int. Ed.* **2021**, *60*, 3229-3237.

[13] M. Crisma, F. Formaggio, C. Toniolo, T. Yoshikawa, T. Wakamyia, *J. Am. Chem. Soc.* **1999**, *121*, 3272-3278.

[14] a) N. Metzler-Nolte, M. Salmain, in *Ferrocenes: Ligands, Materials and Biomolecules* (Ed.: P. Štěpnička), Wiley, Chichester, UK, **2008**, pp. 499-639; b) S. Santi, A. Bisello, R. Cardena, A. Donoli, *Dalton T.* **2015**, *44*, 5234-5257; c) A. Donoli, A. Bisello, R. Cardena, M. Crisma, L. Orian, S. Santi, *Organometallics* **2015**, *34*, 4451-4463.

[15] a) D. N. Van Staveren, N. Metzler-Nolte, *Chem. Rev.* **2004**, *104*, 5931-5985; b) N. Metzler-Nolte, S. I. Kirin, H.-B. Kraatz, *Chem. Soc. Rev.* **2006**, *35*, 348-354; c) L. Barišić, M. Čakić, K. A. Mahmoud, Y. Liu, H.-B. Kraatz, H. S. Pritzkow, I. Kirin, N. Metzler-Nolte, V. Rapić, *Chem. Eur. J.* **2006**, *12*, 4965-4980; d) T. Hirao, *J. Organomet. Chem.* **2009**, *694*, 806-811; e) D. Siebler, M. Linseis, T. Gasi, L. M. Carrella, R. F. Winter, C. Förster, K. Heinze, *Chem. Eur. J.* **2011**, *17*, 4540-4551; f) G. Angelici, M. Górecki, G. Pescitelli, N. Zanna, M. Monari, C. Tomasini, *Biopolymers* **2017**, e23072; g) T. Moriuchi, T. Nishiyama, Y. Tayano, T. Hirao, *J. Inorg. Biochem.* **2017**, *177*, 259-265; h) S. Mehlhose, N. Frenkel, H. Uji, S. Hölzel, G. Müntze, D. Stock, S. Neugebauer, A.

Dadgar, W. Abuillan, M. Eickhoff, S. Kimura, M. Tanaka, *Adv. Funct. Mater.* **2018**, *28*, 1704034.
[16] L. Becucci, I. Guryanov, F. Maran, R. Guidelli *J. Am. Chem. Soc.* **2010**, *132*, 6194–6204.
[17] A. J. Bard, R. Faulkner, Electrochemical methods; Wiley: New York (2001).
[18] O. V. Dolomanov, L. J. Bourhis, R. J. Gildea, J. A. K. Howard, H. Puschmann, *J. Appl. Crystallogr.* **2009**, *42*, 339-341.
[19] G. M. Sheldrick, *Acta Crystallogr.* **2015**, *A71*, 3-8.
[20] G. M. Sheldrick, *Acta Crystallogr.* **2015**, *C71*, 3-8.
[21] C. Amatore, C. Lefrou, F. Pflüger, *J. Electroanal. Chem.* **1989**, *270*, 43-59.

Entry for the Table of Contents

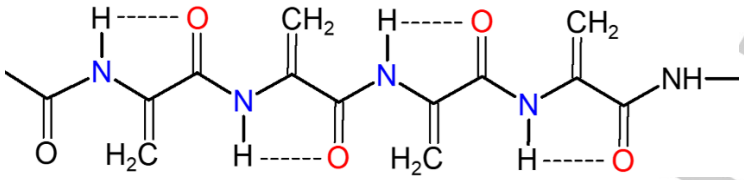

Despite their *flat* and *fully-extended* conformation, $C^{\alpha,\beta}$-didehydroalanine (ΔAla) α-peptide stretches prevent or reduce the charge transfer along the chain, as demonstrated by a joint electrochemical and spectroscopic study exploiting the alternative presence of one ferrocene at the N- or at the C-terminus. Since the macrodipole moment is absent due to the orientation of the carbonyl groups, the peptide length has no influence on the redox behaviour of ferrocene.